Lateral error reduction in the 3D characterization of deep MOEMS devices using white light interference microscopy

Paul Montgomery[(1)], Denis Montaner[(1)], O. Manzardo[(2)] and H.P. Herzig[(2)]

[1]Laboratoire de Physique et Application des Semi-conducteurs (PHASE), CNRS, UPR 292, 23 rue du Loess, 67037 Strasbourg, France, Tel: (33) 03 88 10 62 31, Fax: (33) 03.88.10.62.31,
e-mail: paul.montgomery@phase.c-strasbourg.fr, montaner@phase.c-strasbourg.fr

[2]Institute of Microtechnology, Applied Optics Laboratory, Rue Breguet, 2,
CH-2000, Neuchâtel, Switzerland, Tel: (41) 32 718 3270, Fax: (41) 32 718 3201
e-mail: Omar.Manzardo@unine.ch, HansPeter.Herzig@unine.ch

ABSTRACT

259 words White light scanning interference microscopy is being used increasingly in the rapid 3D characterization of MOEMS micro-systems because of its very high axial resolution over large depths. Although this technique can be used for submicron lateral resolution measurement of critical dimensions on micron high microelectronic structures, recent tests using a standard system have revealed large errors in the lateral measurement of very narrow, deep structures. The use of a Mirau interference objective with the aperture diaphragm of the illumination system fully open in white light has revealed errors in the position of square edges of up to 3 µm. Thus the 2 µm wide, 75 µm deep teeth of an electrostatic comb structure in a FT MOEMS spectrometer appeared to be nearly 7 µm wide. Tests using different types of objectives, with different magnifications, aperture diaphragm values and illumination wavelengths show that the error is greatest for the Mirau objective, with wide aperture diaphragms at longer wavelengths. In addition, the location of the centre of such structures can vary by up to 1 µm depending on the degree of reference mirror tilt.
Investigations of the XZ images of square steps have revealed the presence of "ghost" fringes that can lead to errors in the edge position. Initial studies indicate that these errors are a consequence of a subtle interplay between diffraction effects and the conical illumination. The errors can be considerably reduced using a Linnik type objective with the aperture diaphragm closed down in the presence of shorter wavelength light and the reference mirror perpendicular to the optical axis.

Keywords: 3D characterization, interference microscopy, white light interferometry, MOEMS Microsystems, edge errors.

INTRODUCTION

Following the development and widespread use of micro-electro-mechanical systems (MEMS), the integration of optics in such structures is now an area of considerable growth. Optical MEMS (or MOEMS) technology plays an increasingly important role in domains such as telecommunications, optical networking, information storage, wireless technologies, environmental monitoring, and remote sensing and display technology. Components and systems as varied as the optical bench on a chip, integrated optical laser scanners, micro-shutters or optical switches have been developed at an industrial level. The compatibility with integrated circuit technology allows batch processing and production in large quantities at low cost.
The combination of different technologies on the same device brings with it new challenges for carrying out metrology at both research and production levels. New analytical tools are required that are capable of rapidly and non-destructively

analyzing inhomogeneous materials, on micron or submicron wide structures that may be tens of microns deep and extend over tens of square millimeters.

White light scanning interferometry (WLSI), or Coherence Probe Microscopy (CPM) is being used increasingly for carrying out metrology on such complex structures [1, 2]. The use of far field imaging and a thin virtual scanning probe plane leads to submicron lateral resolution, nanometric axial resolution and the ability to analyze large areas at high speed non-destructively [3, 4, 5, 6]. In previous work [7] a miniature FT spectrometer made with MOEMS technology [8] was investigated using WLSI to explore some of the challenges of carrying out fast, accurate 3D dimensional metrology on such devices. The spectrometer is based on a scanning Michelson interferometer, for use in miniature low cost applications. The system includes narrow (1 µm to 2 µm wide) spring structures and closely interleaved electrostatic combs that are 75 µm in height.

Initial 3D measurements using a typical WLSI configuration consisting of a Mirau interference objective, white light illumination and a modulation contrast detection algorithm resulted in high precision measurement of surface heights. But an artifact was detected concerning the exact lateral location of step discontinuities, which were found to be extended by up to 3 µm. The 1.8 to 2 µm wide comb teeth thus appeared to be up to 7 µm wide. This was surprising since early work on WLSI used for measuring critical dimensions of micron high and wide grating structures demonstrated the possibility of achieving submicron measurement precision (0.010 µm to 0.019 µm) in determining edge location using a high resolution Linnik interferometer with careful calibration [9].

Height artifacts known as "batwings" at the edges of step discontinuities are known to exist for steps lower in height than the coherence length of the light used (typically less than 1 µm) [10, 11], described as being due to diffraction effects at the step discontinuity. But this has not been linked to uncertainties in the edge location.

In this work we have therefore investigated the use of different interference objectives in different optical conditions to try and better understand the problem of lateral artifacts at step discontinuities and to propose some initial solutions to reduce the lateral measurement errors when making full 3D measurements of MOEMS structures.

2. Experimental

2.1 Fabrication of the miniature FT spectrometer MOEMS device

Fourier transform spectroscopy is a well-known and widely used technique in optical metrology. It is a powerful tool for measuring the spectra of weak extended sources, providing a higher signal-to-noise ratio performance compared with other methods. Miniature spectrometers are becoming increasingly attractive for new applications in areas such as color measurement, industrial process control, environmental monitoring and medical diagnostics. To achieve the fabrication of small size, portable sensor solutions, the size and the fabrication cost play an important role in these types of spectrometer.

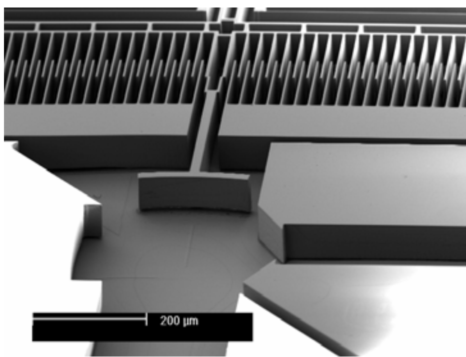

(a) SEM image of sample similar to, but not exactly the same as that measured in the present work ()

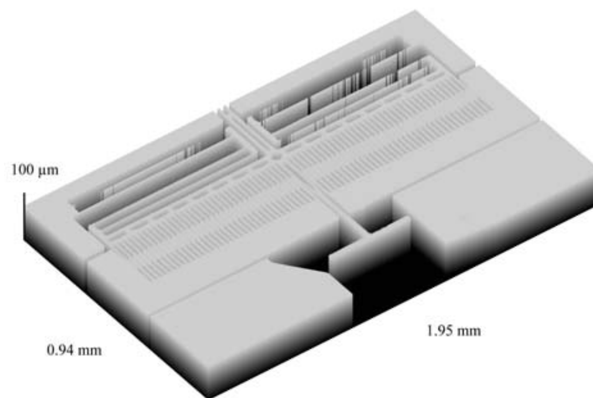

(b) WLSI image of sample used in present work ("stitching" together two images) (2851t52tt shallow3D.jpg)

Fig 1 Overall views of FT spectrometer MOEMS structure

The MOEMS device that has been made (Figure 1) [8] is based on a miniaturized Michelson interferometer used in a time-scanning Fourier transform spectroscopy mode. An electrostatic comb drive actuator moves the scanning mirror through a maximum driving distance of 40 µm. The dimensions of the overall device are 5 mm x 5 mm x 0.5 mm. The measured resolution of the spectrometer is 6 nm at a wavelength of 633 nm.
The actuator and the mirrors are fabricated in a single etch step by deep reactive ion etching (DRIE) of silicon on insulator (SOI) wafers. The actuator is composed of a series of 75 µm high comb electrodes and springs. From SEM images the former were measured to be between 1.8 µm to 2 µm in width and the latter slightly less. Movement is achieved by applying a voltage between the combs. The two opposite comb structures are electrically insulated, one of them being fixed, and the other mechanically connected to the suspension spring. The vertically orientated mirror structure oscillates linearly at a frequency of 1 Hz. The front surfaces of the plasma-etched mirrors are coated with a thin layer of aluminum in order to enhance their reflectivity.
An important aspect of the metrology of such a MOEMS system is the 3D measurement of the different structures in order to determine the process parameters of the etching technique used, and to check the precision that can be achieved. Greater precision in fabrication leads not only to a higher success rate of working modules but also to more uniform performance specifications.

2.2 WLSI measurement system

The WLSI measuring system is based on two different types of microscopes (see details in [2]). The first is a Leitz Linnik microscope with x10 and x50 Linnik objectives (see Table 1 for details), an incandescent lamp and source focus illumination. The second is a Leica DMR-X microscope with x10 and x40 Mirau objectives (see Table 1), a halogen lamp and Köhler illumination. Three narrow band interference filters are available (see Table 2) with centre wavelengths of 632 nm (red), 496 nm (green) and 450 nm (blue). The Mirau objectives, made by Leica, have four positions of reflectivity values (quoted as being 5%, 25%, 50% and 80%) for the reference mirror and a tip/tilt mechanism operated by adjustment screws for orientating the fringes with respect to the plane of the sample. A Sony XC-75E CCD camera with a standard 8 bit digital imaging board are used for image capture and digitalization. The sample is mounted on a piezoelectric transducer (PZT) table with linear feedback (LVDT – linear variable differential transformer) control which has a vertical sensitivity of 10 nm over a range of 100 µm.
The algorithms for system control, image acquisition and image processing were developed in-house. The modulation contrast detection algorithm based on the Five-Sample-Algorithm (FSA [12]) was used "on-the-fly" to measure the full depth of the structure (75 µm) over an image size of 760x572 pixels. To investigate the XZ images and Z profiles at a given position, a full series of 1000 images 128x128 pixels in size were stored in RAM.

3. Measurement results

3.1 MOEMS measurements using a standard WLSI configuration

The following describes measurements made on the MOEMS device using a standard WLSI configuration consisting of the x10 Mirau objective on the Leica DMR-X microscope, with white light and the aperture diaphragm of the illumination system fully open. These are the typical conditions used for making a standard measurement using this technology. Figure 2 shows a close-up portion of the spectrometer near the moving mirror, showing the comb teeth and parts of the suspension spring. As has been well established with this technique [3, 4] the heights of the different structures can be measured to a high precision, in this example to within 100 nm over the full 75 µm depth. Higher axial sensitivity and precision can be obtained using either envelope interpolation or envelope interpolation combined with phase measurement [12]. The greater problem is the presence of lateral errors at step discontinuities. In Figure 2(b) the measured comb teeth can be seen to be much wider than 2 µm, and parts of the slightly narrower spring structures can be observed to be missing at this low magnification (Fig. 2(a)).
Finer analysis of step edges showed that the system was extending the measured position by up to 3 µm, resulting in a false location [7]. Analysis of the XZ intensity images reveals the presence of "ghost" fringes extending out into empty space at the top of the step and inwards underneath the bottom of the step (Figure 3(b)). At a given pixel along the optical axis, Z, the fringe modulation algorithm detects two sets of fringes and selects the one with the greater fringe

modulation as representing the position of the surface. In the middle of the tooth structure and outwards from the tooth edges the choices are obviously correct for defining the top and bottom of the tooth. But near to the edges, the surface positions are false due to the presence of the higher intensity "ghost" fringes at the top of the tooth, leading to a widening in the measured values.

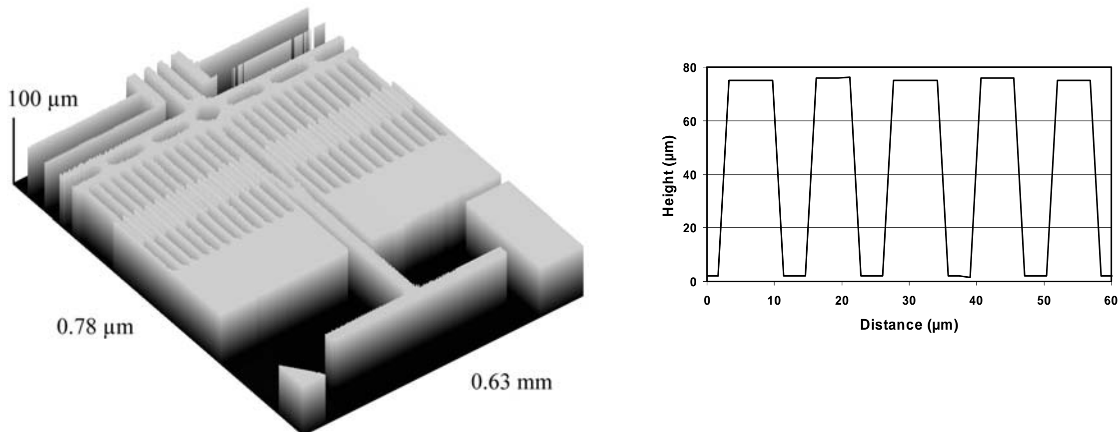

(a) Close-up view by WLSI of mirror, comb teeth and spring structure (2851t52tt shallow cut v2 3D.jpg)

(b) Profile of interleaved comb structure showing widening of teeth (2851.xls)

Fig. 2. Initial measurements of MOEMS spectrometer using standard configuration of WLSI - x10 Mirau objective with aperture diaphragm fully open with white light

3.1 WLSI measurements using different objectives

To better understand the origin of this edge artifact, a series of width measurements of the same comb tooth were carried out using several interference objectives in different optical conditions. The effects of aperture diaphragm, objective type, illumination wavelength and reference mirror tilt were investigated.

The results of the widths of the tooth measured at the half height positions are given in Table 1 for the different objectives and aperture diaphragm openings. Several observations can be made. For the same type of objective, the measured widths are lower for the higher magnification (and larger numerical aperture) and generally lower when the aperture diaphragm is closed down (except in the case of the x10 Mirau). The lowest width measured was 3.04 µm with the x50 Linnik and aperture diaphragm stopped down.

Objective	Numerical aperture	Lateral resolution (µm)	Comb structure width (µm)	
			Aperture diaphragm open	Aperture diaphragm closed
x10 Linnik	0.18	2.07	5.3	3.5
x10 Mirau	0.25	1.49	6.9	7.2
x40 Mirau	0.6	0.62	5.3	5.1
x50 Linnik	0.85	0.44	5.1	3.0

Table 1 Effects of different types of interference objective, magnification and aperture diaphragm opening on measured comb tooth width using WLSI in white light (spectral range 400 nm to 1000 nm)

Normally WLSI is carried out in white light, using the short coherence length of large bandwidth illumination to produce a narrow envelope of fringes. Monochromatic light can be used in WLSI if a large enough numerical aperture objective is used to restrict the spatial coherence of the illumination beam by means of the narrow depth of field [13]. Thus it was possible to test the effects of illumination wavelength of the x40 Mirau objective on the measured tooth width, with the

aperture diaphragm fully open. The results are shown in Table 2. The measured width decreases with wavelength from 6.0 µm at λ = 632 nm to 4.8 µm at λ = 450 nm.

Interference filter	Centre wavelength	Bandwidth	Comb structure width (µm)
Blue	450 nm	39 nm	4.8
Green	496 nm	68 nm	5.7
Red	632 nm	10 nm	6.0

Table 2 Effect of illumination wavelength on the measured comb tooth width using WLSI with the x40 Mirau objective and the aperture diaphragm fully open

3.2 WLSI measurements using a tilted reference mirror

In carrying out these measurements it was found that large variations in measured linewidth were obtained with the Mirau objectives depending on the optical conditions. After investigating various aspects of the optical system it became apparent that the measurements of linear structures with the Mirau objectives were very sensitive to reference mirror tilt about an axis parallel to the structure. The results of tooth width measurements for the x40 Mirau and x50 Linnik objectives with the aperture diaphragm fully open for different reference mirror tilt (approximate values with respect to the optical axis) are given in Table 3. The results for the Linnik objective do not vary significantly with mirror tilt. But for the Mirau objective, the lowest values are found with the mirror perpendicular to the optical axis, the measured width increasing for just slight mirror tilt.
On closer analysis of a single comb tooth structure with the x40 Mirau objective, not only was the measured width found to vary, but its central lateral position was also found to be dependent on the reference mirror tilt. The results of further investigations are shown in Figures 3 and 4. Figure3 shows the XZ images (from the measurement data) after contrast enhancement. These images contain useful information concerning not only the position of interference fringes but also optical distortions. With the tooth being so narrow (2 µm), at the top of the tooth can be seen an approximate view of the 2D longitudinal cross section of the PSF of the system. In Figure 3(b) the "PSF" is symmetrical. With mirror tilt in Figures 3(a) and (c) the "PSF" becomes asymmetrical.

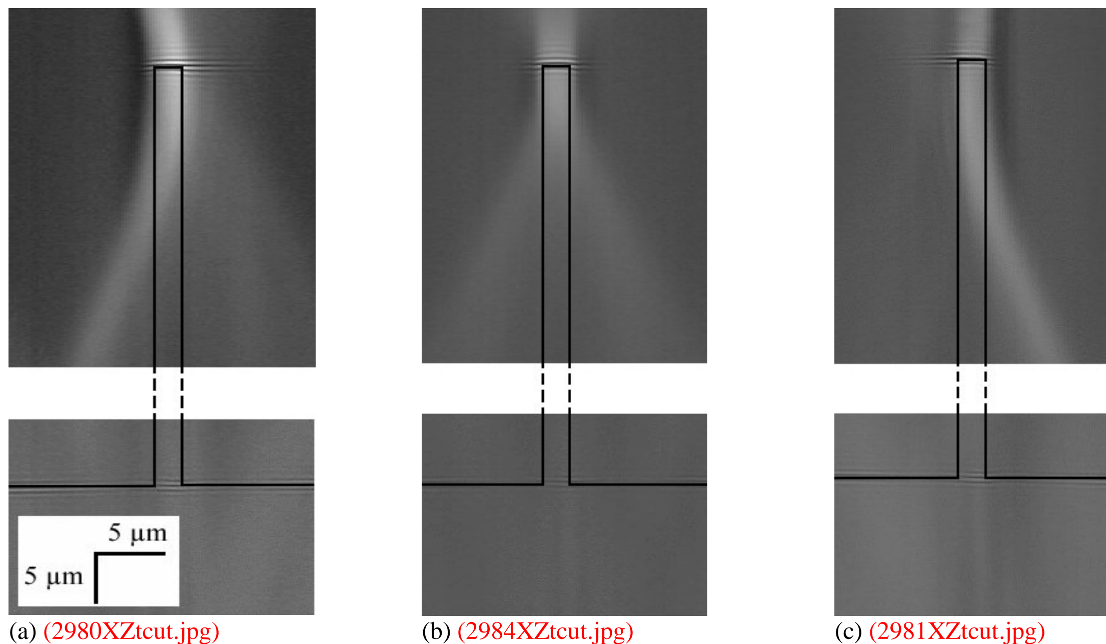

(a) (2980XZtcut.jpg) (b) (2984XZtcut.jpg) (c) (2981XZtcut.jpg)

Fig 3 Contrast enhanced XZ images taken from XYZ image matrices showing presence of "ghost" fringes appearing at the sides of the top and underneath the bottom of the comb teeth measured with the x40 Mirau objective with the aperture diaphragm fully open in white light, with the reference mirror (a) tilted -3° (b) perpendicular and (c) tilted +3° to the optical axis.

Objective	Comb structure width (µm)		
Mirror tilt	-3°	0°	+3°
x40 Mirau	5.2	4.5	6.6
x50 Linnik	3.2	4.2	4.4

Table 3 Effect of reference mirror tilt on measured comb tooth width using WLSI in white light (spectral range 400 nm to 1000 nm) with the aperture diaphragm fully open

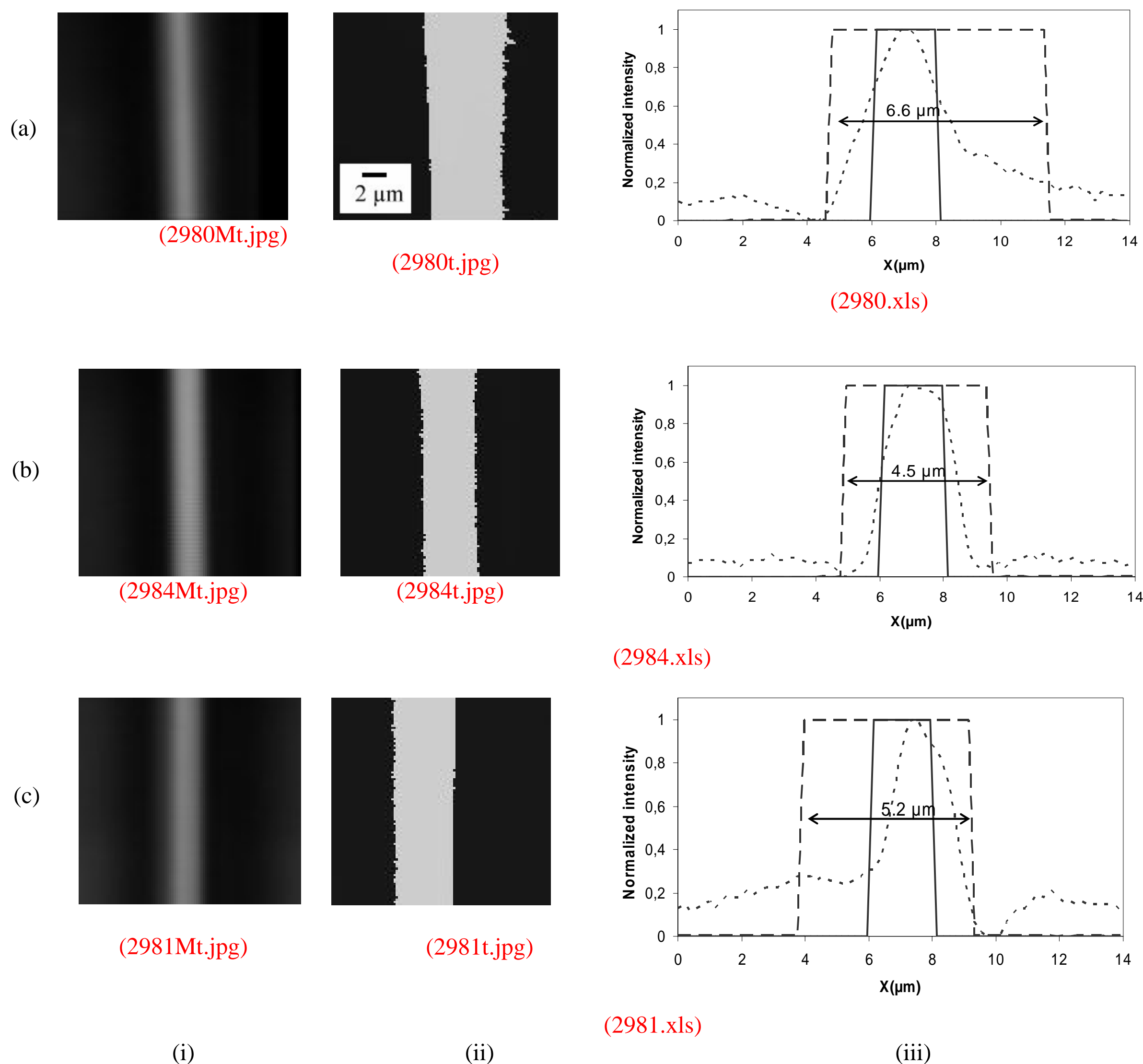

Fig. 4. Measurement data from WLSI with the x40 Mirau objective in white light on the same comb tooth

showing (i) the maximum intensity image, (ii) the height image and (iii) the comparison of profiles (solid line - theoretical shape, dashed line - measured shape, dotted line - intensity profile from XZ image), with the reference mirror (a) tilted at -3° (b) perpendicular and (c) tilted at +3° to the optical axis.

Figure 4 shows various results of the same tooth after processing the XZ image data, showing (a) the maximum intensity images, (b) the height images and (c) profiles of the tooth cross sections for (i) a mirror tilt of -3°, (ii) zero tilt and (iii) a mirror tilt of +3° with respect to the optical axis. Lateral smoothing to remove the effects of noise has not been applied to the height images in (ii), so as to leave the raw data after envelope peak determination of the height positions.
The widening of the measured profiles (Figure 4(b) and (c)) of the teeth results from the presence of the "ghost" fringes observable in Figure 3. In addition, the central positions of the measured structures shifts sideways by up to 1 µm (Figures 4(b) and (c), (i) and (iii)), depending on the sense of the reference mirror tilt. This shift corresponds to the displacement to one side or the other of the "ghost" fringes in Figure 3(a) and (c). Similar measurements made with the x50 Linnik objective did not produce such a sideways shift in the measured position of the teeth nor asymmetry in the "PSF" with reference mirror tilt. This suggests that the errors with the Mirau objective are linked to aberrations in the optical system introduced by tilting the reference mirror. These could arise from the tilt of the transparent plate holding the reference mirror and the semi-transparent front window (see [5]).

3.3 Optimized WLSI measurements of MOEMS

Having demonstrated the existence of measurement errors in the positions of sharp edges of deep structures, and studied some of the properties of the associated "ghost" fringes under different optical conditions, the MOEMS was re-measured using the best conditions available to reduce the errors. These consisted of using the x10 Linnik objective in white light with the aperture diaphragm stopped down and the reference mirror perpendicular to the optical axis. The results (Figure 5) show a big improvement compared with those in Figure 2. The measured comb tooth structures are narrower and the thin suspension spring structures do not having missing measurement points. Using shorter wavelength light would have improved these results further but this was not possible with the Leitz microscope used presently.

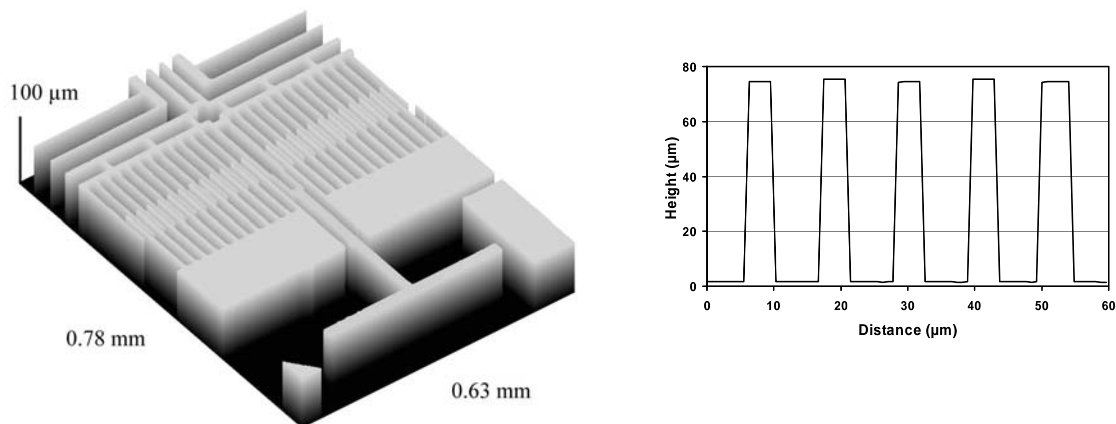

(a) Close-up view by WLSI of mirror, comb teeth and spring structure (2899-2900 bis cut shallow3D.jpg)

(b) Improved profile of interleaved comb structure showing narrower teeth (2899ab.xls)

Fig. 5. Improved measurements of MOEMS spectrometer using modified WLSI - x10 Linnik objective with aperture diaphragm closed down in white light to reduce lateral error measurements

4. Discussion and Conclusions

The use of a standard configuration of WLSI (a Mirau objective in white light with the aperture diaphragm fully open) for the 3D measurement of a deep (75 µm) MOEMS FT spectrometer has revealed the presence of an edge artifact. The measured lateral positions of very square step edges can be up to 3 µm further away from the theoretical position, leading to the measured width of narrow 2 µm wide structures having values of up to 7 µm. In the presence of reference mirror tilt in the Mirau objective, the measured positions of such narrow structures can also be displaced by up to 1 µm from their theoretical lateral positions.
Analysis of the width of a comb tooth structure with different objectives under different optical conditions has shown that these errors can be reduced with the following:

- using larger numerical aperture objectives.
- closing down the aperture diaphragm.
- using shorter average wavelength light.
- in the case of the Mirau objective, keeping the reference mirror perpendicular to the optical axis.
- using the Linnik instead of the Mirau objective.

The greatest errors are introduced by smaller numerical aperture Mirau objectives with the aperture diaphragm fully open with longer average wavelength light in the presence of reference mirror tilt. With the x10 Mirau objective in white light this leads to a measured width of up to 7 µm and a displacement of up to 1 µm sideways. The errors are reduced by using larger numerical aperture Linnik objectives with the aperture diaphragm closed down in shorter wavelength light. With the x50 Linnik objective in white light this leads to a measured width of 3 µm and no onoticeable sideways displacement.
The origin of this problem appears to be due to the presence of "ghost" fringes near to the edge of step discontinuities, leading to an error in the detection of the position of the edge. The position of the edge of the step depends on the selection by the peak detection algorithm of the larger of the two modulation envelopes present, corresponding to the top and bottom of the step. The final selection is a result of a subtle interplay between diffraction effects and the angle of the conical illumination. In the case of the Mirau objective the presence of optical aberrations due to the reference mirror tilt also contribute.

It should be noted that the measurement improvements reported are due solely to modifications in the optical system using a standard fringe envelope detection algorithm and that submicron precisions in step location can be achieved using careful calibration, as in [9].
Further work is being carried out to better understand the exact origin of this artifact and to further improve the lateral measurement precision of the WLSI system in the case of 3D measurement of steps and micron wide structures that are tens of microns in height.

Acknowledgements

The authors would like to acknowledge the financial support of the ACO programme of the CNRS and Rhenaphotonics and to express their thanks to the PHASE laboratory for financial and practical support of this work.

References

[1] R. Windecker, M. Fleischer, K. Körner, H.J. Tiziani, "Testing micro devices with fringe projection and white-light interferometry", *Opt. & Lasers in Eng.,* **36 S**, 141-154, 2001.
[2] M. Flury, A. Benatmane, P. Gérard, P.C. Montgomery, J. Fontaine, T. Engel and J.P. Schunck, "Rapid prototyping of Diffractive Optical Elements (DOEs) for high power lasers using Laser Ablation Lithography fabrication and Coherence Probe Microscopy (CPM) analysis", *Optical Engineering*, **41** (10), 2407-2418, 2002
[3] P. J. Caber, “Interferometric profiler for rough surfaces”, *Appl. Opt.* 32 (1993) 3438.
[4] P. DeGroot and L. Deck, “Surface profiling by analysis of white-light interferograms in the spatial frequency domain”, *J. Mod. Opt.* **42,** 389-401, 1995.
[5] J.P. Fillard. *Near field optics and nanoscopy*, World Scientific, Singapore, 197-214, 1996.

[6] P.C. Montgomery, C. Draman, M. Sieskind, J.P. Ponpon, "Surface morphology analysis of HgI2 and PbI2 with interference microscopy – the challenges of measuring fragile materials and deep surface roughness", *Phys. Stat. Sol. (c)* **0**, 1044-1050, 2003.
[7] P.C. Montgomery, D. Montaner, O. Monzardo, M. Flury and H.P. Herzig, "The metrology of a miniature FT spectrometer MOEMS device using white light scanning interference microscopy", *Thin Solid Films,* **450**, 79-83, 2004.
[8] O. Manzardo, H.P. Herzig, C.R. Marxer, N.F. de Rooij, "Miniaturized time-scanning Fourier transform spectrometer based on silicon technology", *Opt. Letts.* **24**, 1705-1707, 1999.
[9] J.W. Dockrey, D. Hendricks, "The application of coherence probe microscopy for submicron critical dimension linewidth measurement", *Integrated circuit metrology, inspection and process control III*, K.M. Monahan Ed, **1087**, SPIE, Bellingham, Washington, 120-136, 1989.
[10] A. Harasaki, J. Wyant, "Fringe Modulation Skewing Effect in White-Light Vertical Scanning Interferometry" *Appl. Op*t., **39**, 2101-2106, 2000.
[11] A. Harasaki, J. Schmit, J. Wyant, "Improved Vertical-Scanning Interferometry", *Appl. Opt.* **39**, 2107-2115, 2000.
[12] K. G. Larkin, "Efficient nonlinear algorithm for envelope detection in white light interferometry", *J. Opt. Soc. Am.* **A 13**, 832-843, 1996.
[13] P.C. Montgomery, C. Kazmierski and S. BOuchoule, "Submicron profiling using quasi-monochromatic light interferometry", *Inst. Phys. Conf. Series*, **160**, 51-54, 1997.